

**Limits on dark matter WIMPs using upward-going muons in the MACRO detector**

M. Ambrosio,<sup>12</sup> R. Antolini,<sup>7</sup> C. Aramo,<sup>7,a</sup> G. Auriemma,<sup>14,b</sup> A. Baldini,<sup>13</sup> G. C. Barbarino,<sup>12</sup> B. C. Barish,<sup>4</sup> G. Battistoni,<sup>6,c</sup> R. Bellotti,<sup>1</sup> C. Bemporad,<sup>13</sup> E. Bernardini,<sup>2,7</sup> P. Bernardini,<sup>10</sup> H. Bilokon,<sup>6</sup> V. Bisi,<sup>16</sup> C. Bloise,<sup>6</sup> C. Bower,<sup>8</sup> S. Bussino,<sup>14</sup> F. Cafagna,<sup>1</sup> M. Calicchio,<sup>1</sup> D. Campana,<sup>12</sup> M. Carboni,<sup>6</sup> M. Castellano,<sup>1</sup> S. Cecchini,<sup>2,d</sup> F. Ci,<sup>11,13</sup> V. Chiarella,<sup>6</sup> B. C. Choudhary,<sup>4</sup> S. Coutu,<sup>11,e</sup> L. De Benedictis,<sup>1</sup> G. De Cataldo,<sup>1</sup> H. Dekhissi,<sup>2,17</sup> C. De Marzo,<sup>1</sup> I. De Mitri,<sup>9</sup> J. Derkaoui,<sup>2,17</sup> M. De Vincenzi,<sup>14,f</sup> A. Di Credico,<sup>7</sup> E. Diehl,<sup>11</sup> O. Enriquez,<sup>1</sup> C. Favuzzi,<sup>1</sup> C. Forti,<sup>6</sup> P. Fusco,<sup>1</sup> G. Giacomelli,<sup>2</sup> G. Giannini,<sup>13,g</sup> N. Giglietto,<sup>1</sup> M. Giorgini,<sup>2</sup> M. Grassi,<sup>13</sup> L. Gray,<sup>7</sup> A. Grillo,<sup>7</sup> F. Guarino,<sup>12</sup> P. Guarnaccia,<sup>1</sup> C. Gustavino,<sup>7</sup> A. Habig,<sup>3</sup> K. Hanson,<sup>11</sup> R. Heinz,<sup>8</sup> Y. Huang,<sup>4</sup> E. Iarocci,<sup>6,h</sup> E. Katsavounidis,<sup>4</sup> I. Katsavounidis,<sup>4</sup> E. Kearns,<sup>3</sup> H. Kim,<sup>4</sup> S. Kyriazopoulou,<sup>4</sup> E. Lamanna,<sup>14</sup> C. Lane,<sup>5</sup> T. Lari,<sup>2,7</sup> D. S. Levin,<sup>11</sup> P. Lipari,<sup>14</sup> N. P. Longley,<sup>4,i</sup> M. J. Longo,<sup>11</sup> F. Maaroufi,<sup>2,17</sup> G. Mancarella,<sup>10</sup> G. Mandrioli,<sup>2</sup> S. Manzoor,<sup>2,j</sup> A. Margiotta Neri,<sup>2</sup> A. Marini,<sup>6</sup> D. Martello,<sup>10</sup> A. Marzari-Chiesa,<sup>16</sup> M. N. Mazziotta,<sup>1</sup> C. Mazzotta,<sup>10</sup> D. G. Michael,<sup>4</sup> S. Mikheyev,<sup>4,7,k</sup> L. Miller,<sup>8</sup> P. Monacelli,<sup>9</sup> T. Montaruli,<sup>1,l</sup> M. Monteno,<sup>16</sup> S. Mufson,<sup>8</sup> J. Musser,<sup>8</sup> D. Nicoló,<sup>13,m</sup> C. Orth,<sup>3</sup> G. Osteria,<sup>12</sup> M. Ouchrif,<sup>2,17</sup> O. Palamara,<sup>7</sup> V. Patera,<sup>6,h</sup> L. Patrizii,<sup>2</sup> R. Pazzi,<sup>13</sup> C. W. Peck,<sup>4</sup> S. Petreria,<sup>9</sup> P. Pistilli,<sup>14,f</sup> V. Popa,<sup>2,n</sup> A. Rainò,<sup>1</sup> A. Rastelli,<sup>2,7</sup> J. Reynoldson,<sup>7</sup> F. Ronga,<sup>6</sup> A. Sanzgiri,<sup>15,o</sup> C. Satriano,<sup>14,b</sup> L. Satta,<sup>6,h</sup> E. Scapparone,<sup>7</sup> K. Scholberg,<sup>3</sup> A. Sciubba,<sup>6,h</sup> P. Serra-Lugaresi,<sup>2</sup> M. Severi,<sup>14</sup> M. Sioli,<sup>2</sup> M. Sitta,<sup>16</sup> P. Spinelli,<sup>1</sup> M. Spinetti,<sup>6</sup> M. Spurio,<sup>2</sup> R. Steinberg,<sup>5</sup> J. L. Stone,<sup>3</sup> L. R. Sulak,<sup>3</sup> A. Surdo,<sup>10</sup> G. Tarlè,<sup>11</sup> V. Togo,<sup>2</sup> D. Ugolotti,<sup>2</sup> M. Vakili,<sup>15</sup> C. W. Walter,<sup>3</sup> and R. Webb<sup>15</sup>

(MACRO Collaboration)

<sup>1</sup>*Dipartimento di Fisica dell'Università di Bari and INFN, I-70126 Bari, Italy*<sup>2</sup>*Dipartimento di Fisica dell'Università di Bologna and INFN, I-40126 Bologna, Italy*<sup>3</sup>*Physics Department, Boston University, Boston, Massachusetts 02215*<sup>4</sup>*California Institute of Technology, Pasadena, California 91125*<sup>5</sup>*Department of Physics, Drexel University, Philadelphia, Pennsylvania 19104*<sup>6</sup>*Laboratori Nazionali di Frascati dell'INFN, I-00044 Frascati (Roma), Italy*<sup>7</sup>*Laboratori Nazionali del Gran Sasso dell'INFN, I-67010 Assergi (L'Aquila), Italy*<sup>8</sup>*Department of Physics, Indiana University, Bloomington, Indiana 47405**and Department of Physics, Indiana University, Bloomington, Indiana 47405*<sup>9</sup>*Dipartimento di Fisica dell'Università dell'Aquila and INFN, I-67100 L'Aquila, Italy*<sup>10</sup>*Dipartimento di Fisica dell'Università di Lecce and INFN, I-73100 Lecce, Italy*<sup>11</sup>*Department of Physics, University of Michigan, Ann Arbor, Michigan 48109*<sup>12</sup>*Dipartimento di Fisica dell'Università di Napoli and INFN, I-80125 Napoli, Italy*<sup>13</sup>*Dipartimento di Fisica dell'Università di Pisa and INFN, I-56010 Pisa, Italy*<sup>14</sup>*Dipartimento di Fisica dell'Università di Roma "La Sapienza" and INFN, I-00185 Roma, Italy*<sup>15</sup>*Physics Department, Texas A&M University, College Station, Texas 77843*<sup>16</sup>*Dipartimento di Fisica Sperimentale dell'Università di Torino and INFN, I-10125 Torino, Italy*<sup>17</sup>*L.P.T.P., Faculty of Sciences, University Mohamed I, B.P. 524 Oujda, Morocco*

(Received 11 December 1998; published 24 September 1999)

We perform an indirect search for weakly interacting massive particles (WIMPs) using the MACRO detector to look for neutrino-induced upward-going muons resulting from the annihilation of WIMPs trapped in the Sun and Earth. The search is conducted in various angular cones centered on the Sun and Earth to accommodate a range of WIMP masses. No significant excess over the background from atmospheric neutrinos is seen. We set experimental flux limits on the upward-going muon fluxes from the Sun and the Earth. These limits are used to constrain neutralino particle parameters from supersymmetric theory, including those suggested by recent results from DAMA-NaI. [S0556-2821(99)04118-1]

PACS number(s): 95.35.+d, 14.80.-j

<sup>a</sup>Also at INFN Catania, I-95129 Catania, Italy.<sup>b</sup>Also at Università della Basilicata, I-85100 Potenza, Italy.<sup>c</sup>Also at INFN Milano, I-20133 Milano, Italy.<sup>d</sup>Also at Istituto TESRE/CNR, I-40129 Bologna, Italy.<sup>e</sup>Also at Department of Physics, Pennsylvania State University, University Park, PA 16801.<sup>f</sup>Also at Dipartimento di Fisica, Università di Roma Tre, Roma, Italy.<sup>g</sup>Also at Università di Trieste and INFN, I-34100 Trieste, Italy.<sup>h</sup>Also at Dipartimento di Energetica, Università di Roma, I-00185 Roma, Italy.<sup>i</sup>Also at Swarthmore College, Swarthmore, PA 19081.<sup>j</sup>Also at RPD, PINSTECH, P.O. Nilore, Islamabad, Pakistan.

## I. INTRODUCTION

There are many hints pointing to the existence of non-baryonic dark matter in our universe [1], which may consist of *weakly interacting massive particles* (WIMPs). Measurements of the mass density of the universe,  $\Omega_M$ , indicate a density considerably in excess of the density of baryonic matter allowed by big bang nucleosynthesis (BBN) calculations. For example, the POTENT analysis of peculiar velocities of galaxies [2] excludes  $\Omega_M < 0.3$  at the  $2.4\sigma$  level ( $\Omega_M$  is in units of the critical density). In contrast, the limits for baryonic mass ( $\Omega_b$ ) from BBN are  $0.005 \lesssim \Omega_b \lesssim 0.10$  at 95% C.L. [3] for  $0.4 \lesssim h \lesssim 1$ , where  $h$  is the scaled value of the Hubble constant. This discrepancy is an indication that there must be some undiscovered nonbaryonic dark matter. Further, large-scale structure models coupled with Cosmic Background Explorer (COBE) data [4] also favor cosmological scenarios with large amounts of dark matter. One recent model favors a mixture of 70% cold dark matter, 20% hot dark matter and 10% baryons [1]. At smaller scales (roughly 100 to 10 000 kpc) virial estimates on groups and clusters of galaxies and rotation curves of spiral galaxies [5] while requiring smaller values of  $\Omega_M$  are still consistent with the need for non-baryonic dark matter. Furthermore, dark matter in galaxies is also motivated by the fact that dark matter halos seem to help stabilize spiral disk structure [6]. Even with the inclusion of massive compact halo objects (MACHOs) into this picture we are still unable to account for all of the dark matter halo of our galaxy [7].

A long list of nonbaryonic cold dark matter candidates has been suggested, among which the supersymmetric (SUSY) neutralino, considered in this paper, and the axion seem to be the most promising [8]. SUSY postulates a symmetry between bosons and fermions predicting SUSY partners to all known particles (for a review see Ref. [9]). SUSY solves a host of particle physics questions such as the ‘‘hierarchy problem’’ [explaining the large difference between the weak and grand unified theory (GUT) scales]; generating electroweak symmetry breaking through the Higgs boson mechanism; and stabilizing the Higgs boson mass at the weak scale. In theories where  $R$  parity is conserved there exists a stable lightest supersymmetric particle (LSP). If the neutralino is the LSP it is a natural WIMP candidate: it is a weakly interacting particle with a mass between roughly a GeV and a TeV and would be expected to have a significant relic density. The neutralino  $\tilde{\chi}$  is the lightest linear superposition of gaugino and Higgsino eigenstates (gauginos and Higgsinos are SUSY counterparts to the Higgs and gauge bosons):

$$\tilde{\chi} = a_1 \tilde{\gamma} + a_2 \tilde{Z} + a_3 \tilde{H}_1 + a_4 \tilde{H}_2, \quad (1.1)$$

where  $\tilde{\gamma}$  and  $\tilde{Z}$  are gaugino states and  $\tilde{H}_1$  and  $\tilde{H}_2$  are Higgsino states.

Currently, supersymmetric parameter space for the neutralino is constrained primarily by accelerator searches. Data from the CERN  $e^+e^-$  collider LEP [10] lead to lower limits on the neutralino mass  $m_\chi$  between 20 and 30 GeV. These limits are model dependent and correlated to limits from chargino (a mixture of  $w$ -inos and charged Higgsinos) searches.

In this framework, ‘‘direct’’ and ‘‘indirect’’ methods for detecting Galactic halo WIMPs can probe complementary regions of the supersymmetric parameter space, even when more extensive LEP 2 results become available. Direct methods detect WIMPs via a direct interaction of a WIMP, such as by observing the energy deposited in a low-background detector (e.g., semiconductors or scintillators) when a WIMP elastically scatters from a nucleus. Indirect methods look for by-products of WIMP decay or annihilation such as neutrinos resulting from the annihilation of WIMPs. An excellent prospect for indirect WIMP searches is to look for high energy neutrinos from WIMP annihilation in the core of the Earth or the Sun [11–13]. In MACRO, such neutrinos would be detected as neutrino-induced upward-going muons which can be distinguished from downward-going cosmic-ray shower muons.

## II. UPWARD-GOING MUONS FROM WIMP ANNIHILATION

Dark matter WIMPs in the Galactic halo can be captured in a celestial body by losing energy through elastic collisions and becoming gravitationally trapped. As the WIMP density increases in the core of the body, the WIMP annihilation rate increases until equilibrium is achieved between capture and annihilation. High energy neutrinos are produced via the hadronization and decay of the annihilation products (mostly fermion-antifermion pairs, weak and Higgs bosons) and may be detected as upward-going muons in underground detectors.

The capture rate for an astrophysical body depends on several factors: the WIMP mean halo velocity ( $\sim 270 \text{ km s}^{-1}$ ), the WIMP local density ( $\rho_\chi \sim 0.3 - 0.6 \text{ GeV cm}^{-3}$ ), the WIMP scattering cross section, and the mass and escape velocity of the celestial body [8]. The WIMP may scatter from nuclei with spin (e.g., hydrogen in the Sun) via an axial-vector (‘‘spin-dependent’’) interaction in which the WIMP couples to the spin of the nucleus or via a scalar interaction in which the WIMP couples to the nuclear mass. In axial-vector interactions the probability for a given energy loss is constant up to the kinematic limit of the interaction, while for a scalar interaction there will be a suppression of the cross section at high momentum transfers [8]. Elastic scattering is most efficient when the mass of the WIMP is similar to the mass of the scattered nucleus. Hence, the heavy nuclei in the Earth make it very efficient in capturing WIMPs with  $m_\chi \lesssim 100 \text{ GeV}$  (the resonance effect [14]). The Sun, in contrast, has a smaller average nuclear mass, but is nonetheless efficient in capturing WIMPs due to its larger escape velocity.

<sup>k</sup>Also at Institute for Nuclear Research, Russian Academy of Science, RU-117312 Moscow, Russia.

<sup>l</sup>Corresponding author E-mail: montaruli@ba.infn.it

<sup>m</sup>Also at Scuola Normale Superiore di Pisa, I-56010 Pisa, Italy.

<sup>n</sup>Also at Institute for Space Sciences, 76900 Bucharest, Romania.

<sup>o</sup>Also at Tektronix Inc., Wilsonville, OR 97070.

A WIMP annihilation signal would appear in an underground experiment as a statistically significant excess of upward-going muon events from the direction of the Sun or of the Earth among the background of atmospheric neutrino-induced upward-going muons. High energy neutrino-induced upward-going muons tend to retain the directionality of the parent neutrino. This directionality permits a restriction of the search for WIMP annihilation neutrinos to a narrow cone pointing from the Earth or Sun, greatly reducing the background from atmospheric neutrinos. This effect, along with the increase in neutrino cross section with energy and longer range of high energy muons, means that this method of detection achieves an increasingly better signal to noise ratio for high WIMP masses.

Data on upward-going muons from the core of the Earth and of the Sun have been presented by several experiments, notably Baksan [15], Kamiokande [16], and IMB [17]. In this paper we describe a WIMP search using the MACRO detector.

### III. WIMP SEARCH IN MACRO FROM THE EARTH AND THE SUN

The MACRO apparatus [21], located in the Gran Sasso Underground Laboratory of the Italian Istituto Nazionale di Fisica Nucleare, detects upward-going muons using a system of limited streamer tubes for tracking (angular resolution  $\sim 0.5^\circ$ ) and roughly 600 tons of liquid scintillator for fast timing (time resolution  $\sim 500$  ps). The detector has overall dimensions of  $12 \times 77 \times 9$  m<sup>3</sup> and it is divided in 6 units called *supermodules*. The bottom 4.8 m of the apparatus is filled with rock absorber along with active detector elements which sets a minimum energy threshold of about 1 GeV for vertical muons crossing the detector. The upper part, called the *attico*, is an open volume containing electronics as well as active detector elements. The streamer tubes form 14 horizontal and 12 vertical planes and the liquid scintillator counters form 3 horizontal and 4 vertical planes on the outer surfaces of the detector.

The neutrino events in the MACRO detector used for the WIMP search can be seen in two different topologies

(1) Through-going upward muons. These events are produced by neutrinos interacting in the rock below MACRO and pass entirely through the detector. For atmospheric neutrinos the spectrum ranges from 1 to  $10^4$  GeV and the peak energy is about 100 GeV.

(2) Internally produced upward-going events induced by neutrinos interacting in the lower part of the detector and producing a lepton which moves upward through the two upper scintillator layers. For atmospheric neutrinos the peak energy is about 4 GeV. To detect these events the *attico* must be in operation. For atmospheric neutrinos the peak energy is about 4 GeV.

These topologies are recognized using the time-of-flight technique. The time-of-flight technique is used to discriminate upward-going neutrino-induced muons from the background of downward-going atmospheric muons. Each scintillator records the time of a particle crossing by measuring the mean time at which signals are observed at the two ends

of the counter. The transit time of a particle is found by taking the difference between the crossing times of two scintillation counters. In our convention, upward-going muons are considered to have a negative velocity, and downward-going muons a positive velocity.

We present the results of WIMP searches using data gathered from March 1989 to March 1998. This data set encompasses five years of running with partial apparatus (March 1989 to April 1994) and 4 years of running with the full apparatus including the *attico* (April 1994 to March 1998) and it corresponds to livetimes including efficiency of 1.38 yr of running with the first supermodule, 0.41 yr of running with the lower part of the detector, and 3.1 yr of running of the full detector. The details of the upward-going muon analysis for the first supermodule and the lower detector can be found in Ref. [22], for the full apparatus in Ref. [23].

#### A. The search for WIMPs from the Earth

Slightly different data sets and selection criteria are used for the WIMP searches for the Earth and the Sun in order to optimize the signal over background for each. For the Earth analysis only through-going upward muons which traverse at least  $200$  g/cm<sup>2</sup> of absorber are used (category 1 above). The absorber requirement reduces the background due to soft pions produced at large angles by undetected downward-going muons to 1% [24]. A total of 517 through-going upward muon events are used in the search for WIMP annihilation neutrinos from the Earth. We consider several contributions to the background of through-going upward muons: events with an incorrect timing measurement (such as muons in coincidence with radioactivity, other muons, or electromagnetic showers) and soft pions produced at large angles. We estimate 20 background events in the Earth sample of 517 through-going upward muons.

The expected background of upward-going muons from atmospheric neutrinos is calculated with a full Monte Carlo calculation (described in Refs. [22,23]). This calculation uses the Bartol flux [25], the Morfin and Tung parton set  $S_1$  [26] for the deep inelastic  $\nu N$  cross-section, and the muon energy loss in the rock from Ref. [27]. We estimate a total uncertainty in the calculation of 17% [22,23]. We have considered scenarios both with no neutrino oscillations as well as with the neutrino oscillation parameters of Ref. [23]. The oscillations parameters considered are  $\Delta m^2 = 2.5 \times 10^{-3}$  eV<sup>2</sup> and  $\sin^2 2\theta = 1$  and the statistical significance of the agreement between the data and the oscillation model considered is discussed in Ref. [23].

In the no-oscillation scenario the expected number of atmospheric neutrino events is  $662 \pm 113_{\text{theor}}$  as compared to  $462 \pm 79_{\text{theor}}$  in the oscillation scenario. In both cases there is a deficit of the measured events with respect to the expected number in the region around the vertical direction of MACRO, where the efficiency and acceptance of the apparatus are best known. This has been checked using the large statistics of downward-going muons. Particularly, we have compared the acceptance and efficiency evaluation of the upward-going muon analysis with the analysis of the vertical muon intensity [28] and in the vertical region they are in agreement within 5%.

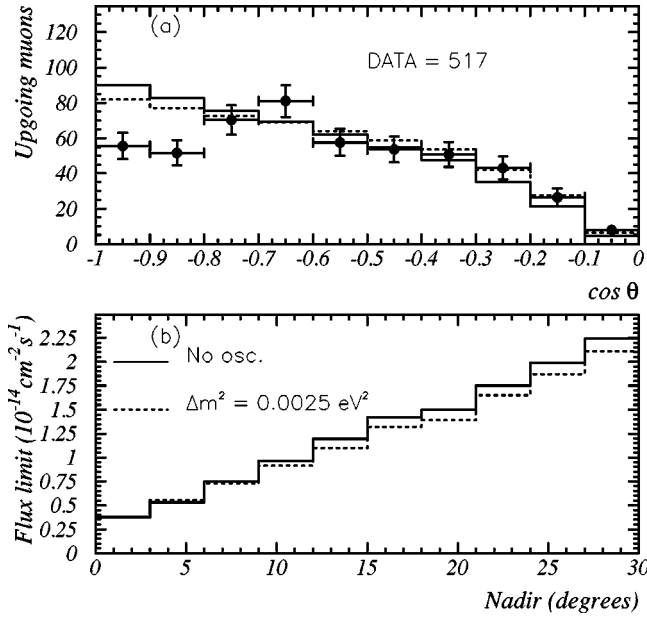


FIG. 1. (a) Distribution of measured through-going upward muons (black circles) as a function of the cosine of the zenith angle ( $\theta$ ). The expected distribution of through-going upward muons induced by atmospheric neutrinos are shown for the no oscillation and the  $\nu_\mu - \nu_\tau$  oscillation hypothesis for maximum mixing and  $\Delta m^2 = 0.0025 \text{ eV}^2$  (solid line and dashed line). The expected distributions are multiplied by the ratio of the measured events over the expected ones outside the largest window ( $30^\circ$ ). The normalization factors are 0.82 for the solid line and 1.19 for the dashed line. (b) Muon flux limits (90% C.L.) as a function of the search cone which is the angle from the vertical (the nadir angle). The angle varies from  $3^\circ$  to  $30^\circ$  in steps of  $3^\circ$ . In both plots, the dashed line is obtained in the hypothesis of  $\nu_\mu \rightarrow \nu_\tau$  oscillations of the atmospheric neutrino background with maximum mixing and  $\Delta m^2 = 0.0025 \text{ eV}^2$ .

Because of the discrepancy between the observed and expected numbers of upward-going muons in the expected signal region ( $0^\circ$  to  $30^\circ$  from the vertical), we normalize the expected signal using data outside the expected signal region. This normalization is motivated by the fact that the absolute error of the expected flux is relatively high, whereas the shape of the flux is known to a few percent [29]. This normalization factor is determined separately for each of the search cones considered, using the ratio of observed to expected events outside the search cone.

We show both the expected atmospheric neutrino background with and without oscillations in Figs. 1(a) and 1(b). Figure 1(a) shows the zenith angle distribution of the measured events and of the expected ones from atmospheric neutrinos. If neutrinos oscillate with these parameters the expected number of events would be reduced and the angular distribution of through-going upward muons would be distorted because neutrinos at the nadir oscillate more than those at the horizon due to their longer pathlength (for a full discussion see Ref. [23]). We note that the slight excess observed in the region  $-0.7 \leq \cos \theta \leq -0.6$  is very unlikely to be produced by any plausible WIMP model, since this region

is far from the expected signal region [ $\theta \lesssim 30^\circ$ —see Fig. 3(a)].

Muon flux limits are evaluated as

$$\Phi(90\% \text{ C.L.}) = \frac{N_{\mathcal{P}}(90\% \text{ C.L.})}{\mathcal{E}}, \quad (3.1)$$

where  $N_{\mathcal{P}}$  is the upper Poissonian limit (90% C.L.) given the number of measured events and expected background [30] due to atmospheric neutrinos and  $\mathcal{E}$  is the exposure given by equation

$$\mathcal{E} = \int_{T_{\text{start}}}^{T_{\text{end}}} \epsilon(t) \times A[\Omega(t)] dt, \quad (3.2)$$

where  $A[\Omega(t)]$  is the detector area in the direction of the expected signal ( $\Omega$ ) at time  $t$ ,  $\epsilon$  is the detector efficiency (discussed in Refs. [22,23]) which takes into account the possible variations of detector running configuration during data taking, and  $T_{\text{start}}$  and  $T_{\text{end}}$  are the start and end times of data taking. For the Earth, the signal is expected always from the same direction, hence  $\Omega$  is a constant with time and the detector acceptance  $A$  is calculated using the Monte Carlo calculation in Refs. [22,23], the live-time and efficiency are calculated using downward-going events.

Since the number of detected events is less than that expected from the atmospheric neutrino flux, we set conservative flux limits by assuming that the number of measured events in the signal region equals the number of expected events in that region [30]. In Fig. 1(b) the 90% C.L. muon flux limits for the Earth are plotted as a function of the nadir angle for 10 search half-cones around the vertical from  $3^\circ$  to  $30^\circ$ . For this data, the average value of the exposure is  $2620 \text{ m}^2 \text{ yr}$  (it varies slightly for different search cones because the area decreases by  $37 \text{ m}^2$  when the search cone increases from  $3^\circ$  to  $30^\circ$  around the vertical). Note that the flux limits are independent of any hypothesis concerning a WIMP signal (or any other source). As shown in Fig. 1(b), the application of a  $\nu_\mu - \nu_\tau$  oscillation hypothesis to the atmospheric neutrino background with  $\Delta m^2 = 0.0025 \text{ eV}^2$  and maximum mixing will result in lower flux limits. The flux limits for the Earth are presented in Table I as a function of the angle of the search cone.

## B. The search for WIMPs from the Sun

Background rejection is not so critical for moving sources as it is for steady sources, as a result the analysis for the Sun does not require that a minimum of absorber thickness be crossed as did the one for the Earth. Hence, the Sun data sample includes through-going upward muons with no absorber requirement as well as semicontained events generated in the lower half of the detector (category 2 above), for a total of 762 upward-going muon events. Apart from this, the analysis for the Sun is basically the same as the one for the Earth.

In the analysis for muons pointing in the direction of the Sun, the data themselves are used to generate the expected

TABLE I. Observed and background events and 90% C.L. muon flux limits for some of the 10 half cones chosen pointing from the Earth and the Sun. The background events are those expected from atmospheric neutrinos. In the case of the Earth, the normalization factors are used to normalize the expected background events by the ratio of observed to expected events outside each cone. Since the number of detected events (column 2) is less than the normalized expected events (column 3), we set conservative flux limits assuming that the number of measured events equals the number of expected ones [30]. The Earth results are for the no oscillation scenario. Earth limits considering neutrino oscillations agree to within 8%. The average exposure for the Earth is 2620 m<sup>2</sup> yr and for the Sun 890 m<sup>2</sup> yr.

Cone	Earth			Sun			
	Data	Back-ground events	Norm. factor	Flux Limit ( $E_\mu > 1.5$ GeV) ( $\text{cm}^{-2} \text{s}^{-1}$ )	Data	Back-ground events	Flux Limit ( $E_\mu > 2$ GeV) ( $\text{cm}^{-2} \text{s}^{-1}$ )
30°	76	119.2	0.82	$2.24 \times 10^{-14}$	56	51.8	$5.84 \times 10^{-14}$
24°	52	75.5	0.79	$1.75 \times 10^{-14}$	33	33.1	$3.83 \times 10^{-14}$
18°	32	42.2	0.77	$1.42 \times 10^{-14}$	17	18.8	$2.60 \times 10^{-14}$
15°	24	29.0	0.76	$1.20 \times 10^{-14}$	11	13.2	$2.09 \times 10^{-14}$
9°	10	10.5	0.75	$7.48 \times 10^{-15}$	3	4.7	$1.34 \times 10^{-14}$
6°	4	4.6	0.75	$5.30 \times 10^{-15}$	2	2.1	$1.37 \times 10^{-14}$
3°	0	1.1	0.75	$3.79 \times 10^{-15}$	2	0.5	$1.73 \times 10^{-14}$

events in order to properly include the effects of semicon- tained events. The arrival times from measured downward- going muons from the entire period of data taking are as- signed randomly to the local trajectory coordinates of the measured upward-going muon events to evaluate their right ascension. This procedure allows us to take into account drifts of detection efficiency in time. Figure 2(a) shows the angular distributions of measured and expected upward- going muons with respect to the direction of the Sun. The shape depends on the seasonal variation of the position of the Sun and on the lifetime of the apparatus. The upward-going events detected during the night fall towards a cosine of 1, while the events collected during the day fall near  $-1$ . The exposure of the Sun is calculated with Eq. (3.2) using the detector acceptance from the Monte Carlo described in Ref. [23] (for  $E_\mu > 2$  GeV, see below). The dependence of the acceptance of the detector on the direction of the Sun when it is below the horizon is calculated using both the Monte Carlo and downward-going muon data. Flux limits are calculated using Eq. (3.1). In Fig. 2(b) the flux limits (90% C.L.) for an exposure of  $\sim 890$  m<sup>2</sup> yr (it varies slightly for different search cones) for 10 search cones around the Sun direction are shown. Again, it should be noted that any neu- trino oscillation effects are automatically included in our method of deriving the number of expected events from real data.

Table I shows the number of detected and expected upward-going muon events and corresponding flux limits for several cone sizes for the Earth and Sun. The muon threshold energy is determined by the amount of absorber an upward- going muon must traverse in MACRO. It is lower for the Earth (where tracks are oriented towards the vertical) than it is for the Sun (where tracks are more inclined). The upper limits in Table I are calculated assuming a minimum energy of 1.5 and 2 GeV for the Earth and the Sun, respectively. Given the analysis requirements to select upward-going muons above these energies, we make a maximum error of

5% with respect to an exact calculation which takes into account the dependence on energy of the acceptance of the apparatus and of the neutrino fluxes from neutralinos with different masses.

#### IV. FLUX LIMITS COMPARED TO SUSY PREDICTIONS

The flux limits from the previous section can be used to constrain any WIMP model. There are many calculations of the expected neutrino fluxes from WIMP capture and anni- hilation in the Sun and Earth [8,18,19]. However, before we

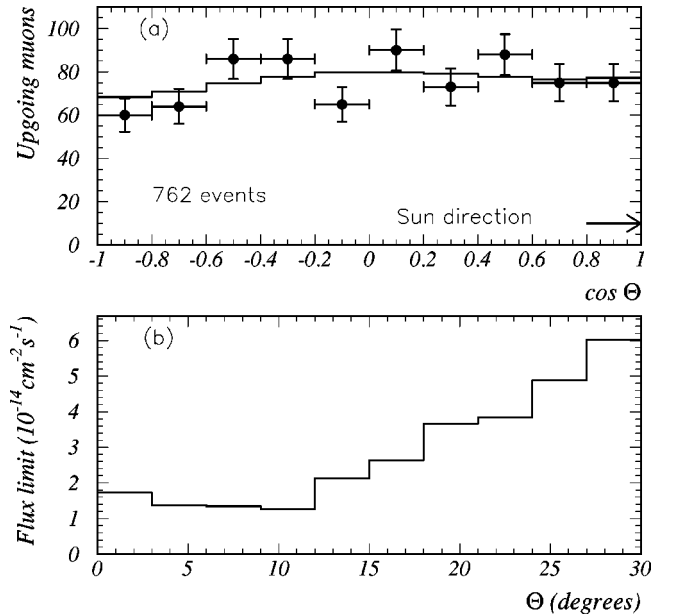


FIG. 2. (a) Distribution of measured upward-going muons (black circles) and of the expected upward-going muons induced by atmospheric neutrinos (solid line) as a function of the cosine of the angle from the Sun direction. (b) Muon flux limits (90% C.L.) as a function of the search cone around the direction of the Sun.

can carry out such a comparison it is helpful to discuss some of the details of these models. In order to compare our experimental results, we have considered calculations developed in the frame of the minimal supersymmetric extension of the standard model (MSSM).

If the minimal supersymmetric extension of the standard model [8] is coupled with some GUT assumptions ( $M_1 = 5/3 M_2 \sin^2 \theta_W$  where  $\theta_W$  is the Weinberg angle), then the neutralino mass depends on a few supersymmetric parameters: one of the two gaugino mass parameters,  $M_1$  or  $M_2$ , the Higgsino mass parameter  $\mu$ , and the ratio of the Higgs doublet vacuum expectation values,  $\tan \beta$ . The phenomenology of neutralinos is determined by the composition parameter  $P = a_1^2 + a_2^2$ . Some other parameters must be determined in order to define the processes induced by neutralinos, because Higgs and the supersymmetric partners of fermions (sfermions) play a relevant role. In the MSSM there are two Higgs doublets, hence three neutral Higgs fields (two scalar and one pseudoscalar). The Higgs sector is determined by two independent parameters:  $\tan \beta$  and  $m_A$ , the mass of the pseudoscalar neutral boson. The other parameters in the Lagrangian of the model are the bilinear and trilinear parameters connected to the spontaneous symmetry breaking. The number of parameters needed to describe neutralino phenomenology may be reduced further by assuming that all the trilinear parameters are zero except for the third family, which are assumed to have the common value  $A$  and that all the squarks and sleptons are degenerate with common mass  $m_0$ .

The models are generally developed taking into account the experimental constraints on the parameter space coming from colliders [10] and from the measurement of the  $b \rightarrow s \gamma$  process. The experimental result we present in this paper can be used to constrain any of the developed calculations. Here we have compared our result with the Bottino *et al.* model [18,20]. Another model we have considered is the one by Bergström *et al.* [19]. The main difference between these two models is how they deal with configurations of low values of the neutralino cosmological abundance ( $\Omega_\chi h^2 < 0.025$ ). For the calculations of upward-going muons from neutralino annihilation, Bergström *et al.* does not consider these configurations. On the other hand, Bottino *et al.*, when the neutralino cosmological abundance is too low to account for the total dark matter in the halo, assume

$$\text{if } \Omega_\chi h^2 > (\Omega h^2)_{\min} \quad \rho_\chi = \rho_{\text{loc}}, \quad (4.1)$$

$$\text{if } \Omega_\chi h^2 < (\Omega h^2)_{\min} \quad \rho_\chi = \rho_{\text{loc}} \times \Omega_\chi h^2 / (\Omega h^2)_{\min}.$$

where  $(\Omega h^2)_{\min} = 0.03$  and  $\rho_{\text{loc}} = 0.5 \text{ GeV cm}^{-3}$ . These configurations are still compatible with experimental limits, with both calculations yielding consistent predictions for high values of  $\Omega_\chi h^2$ . Moreover, both calculations indicate that indirect searches will have sensitivities at high neutralino masses. In this section, we will make the comparison between our data and the predictions of the neutralino models of Bottino *et al.* [20] using search cones which collect 90% of the expected signal.

The angular distribution of upward-going muons follows that of the parent neutrinos, with deviations due to charged-current neutrino interaction and Coulomb multiple scattering of the produced muons on their path to the detector. Both of these distributions are a function of the neutrino energy. In turn, the energy spectrum of neutrinos produced in WIMP annihilation depends both on the WIMP mass and the annihilation products. The final states can be pairs of fermions, or Higgs/gauge bosons or combinations of Higgs and gauge bosons. The branching ratios into these channels depend on the model and they have some effect on the neutrino energy spectra. Annihilation to fermion pairs tends to produce softer neutrinos than annihilation to gauge bosons since fermions dissipate energy in hadronization whereas bosons have a greater likelihood of prompt decay to neutrinos. We estimate the maximum variation in flux limits by taking the extreme cases where only one annihilation channel is open. We find this variation is no more than 17% between extreme models and those considered here. To a good approximation, the angular distribution is a function of just the neutralino mass, and so we determine flux limits as a function of neutralino mass.

The angular distributions of the upward-going muon signals are calculated using neutrino fluxes from neutralino annihilation in the Sun and Earth calculated by Bottino *et al.* [20]. A Monte Carlo calculation with cross sections described in Ref. [31] and muon energy loss as described in Ref. [32] is used to propagate muons through the detector where the angular resolution is taken into account.

The main difference between the angular distributions of the signals from Earth and Sun is due to the angular resolution of the detector which degrades for slanted tracks because the number of streamer tube layers crossed decreases. Hence, the more slanted tracks from the Sun tend to have lower angular resolution than those from the Earth. Moreover, the angular size of the expected signal is affected by the angular size of the region where WIMP annihilation is taking place. The diameter of the Sun is  $0.5^\circ$  (as seen by the Earth) and the WIMPs are expected to be localized at the center of the Sun. As a result, the angular size of the WIMP annihilation region is negligible. However, for the Earth the angular size of the annihilation region is considerable and has been estimated by [33,14,18] to be

$$G(\theta) \simeq 4m_\chi \alpha e^{-2m_\chi \alpha \sin^2 \theta} \quad (4.2)$$

where  $\theta$  is the nadir angle,  $\alpha$  is a parameter depending on the central temperature ( $T = 6000 \text{ K}$ ), the central density ( $\rho = 13 \text{ g cm}^{-3}$ ), and the radius of the Earth ( $\alpha = 1.76 \text{ GeV}^{-1}$ ).

In Fig. 3 the muon nadir angle is shown for  $m_\chi = 60, 100, 200, 500,$  and  $1000 \text{ GeV}$  and fixed model parameters. In Fig. 4 the angular spreads between the neutrino and the muon directions are shown as a function of neutralino mass in the case of the search for neutralinos trapped inside the Sun.

The 90% C.L. flux limits are calculated as a function of neutralino mass using cones which collect 90% of the expected signal. These limits are corrected for the 90% collec-

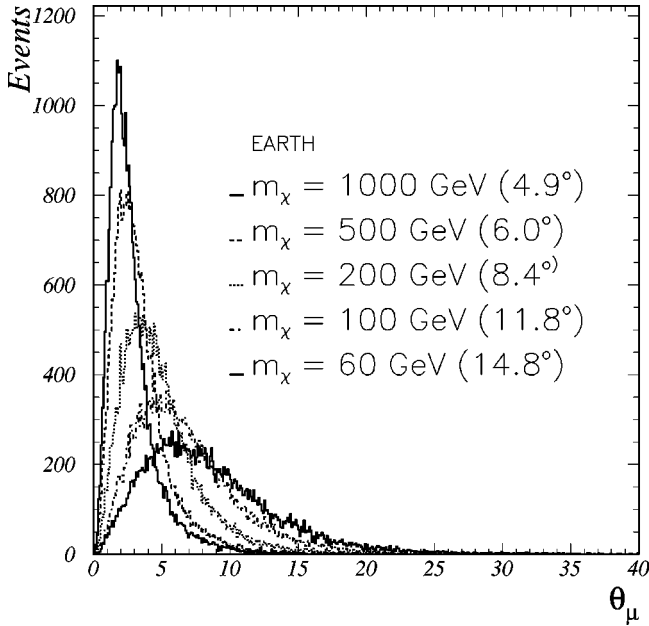


FIG. 3. Nadir angle distribution of muons induced by neutralino annihilation inside the Earth for several neutralino masses. The curves are the result of the simulation described in Sec. IV. The more peaked distributions correspond to the higher masses considered. The angular ranges including 90% of the signal are indicated.

tion efficiency due to cone size. Figures 5 and 6 show these limits for the Earth and Sun, respectively. The experimental limits are superimposed on the flux of upward-going muons from the Bottino *et al.* calculation as a function of  $m_\chi$ . The flux limits are calculated for the same muon minimum en-

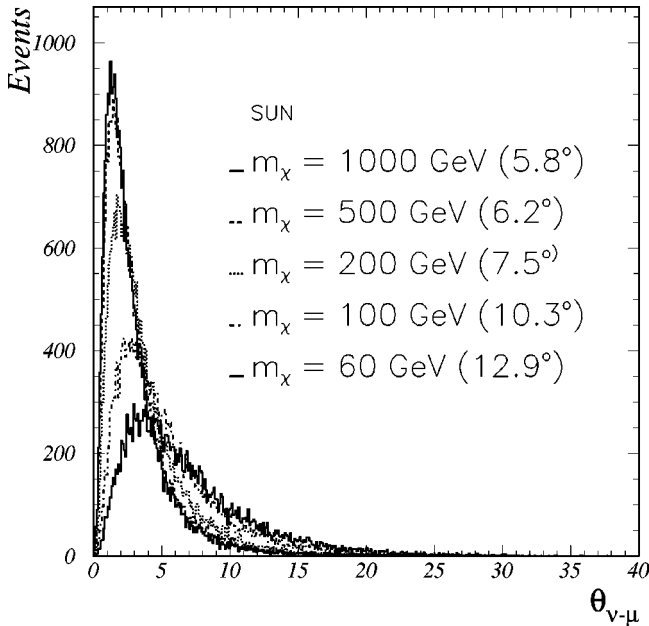


FIG. 4. Neutrino-muon angular separation distribution for neutralinos from  $\tilde{\chi}-\tilde{\chi}$  annihilation in the Sun for several neutralino masses. The more peaked distributions correspond to the higher masses considered. The angular ranges with 90% of the signal are shown.

ergy as is used in the calculation ( $E_\mu > 1$  GeV) considering the dependence on the energy of the MACRO acceptance in the low energy region. A correction is applied for each neutralino mass to translate from the thresholds of Table I to the 1 GeV threshold used in the calculation of upward-going muon fluxes. The correction factors are higher for lower neutralino masses. Moreover, they are higher for the Sun for which the threshold in Table I is 2 GeV than for the Earth for which it is 1.5 GeV. We estimate these factors to be 1% for the Earth and 10% for the Sun for a neutralino mass of 60 GeV.

The fluxes are calculated by varying the model parameters (each model is represented by a dot in Figs. 5 and 6) in the following experimentally allowed ranges:  $1 \leq \tan \beta \leq 50$ ,  $65 \text{ GeV} \leq m_A \leq 500 \text{ GeV}$ ,  $150 \text{ GeV} \leq m_0 \leq 500 \text{ GeV}$ ,  $-3 \leq A \leq 3$ ,  $20 \text{ GeV} \leq |\mu| \leq 500 \text{ GeV}$ . The calculation also assumes a neutralino rms halo velocity of  $270 \text{ km s}^{-1}$ , a halo escape velocity of  $650 \text{ km s}^{-1}$ , a velocity of the Sun around the Galactic center of  $232 \text{ km s}^{-1}$ , a local dark matter density of  $0.5 \text{ GeV cm}^{-3}$ , and a minimal value for rescaling the neutralino relic abundance  $(\Omega h^2)_{\min}$  of 0.03 (explained above). Those fluxes lying above the experimental flux limit curve are ruled out as possible SUSY models by this measurement given the cosmological parameters chosen. It should be noted that a variation of the astrophysical parameters used in these flux predictions may lower the calculated fluxes by at most one order of magnitude [20]. Moreover,  $\nu_\mu - \nu_\tau$  oscillations could lower neutrino fluxes from neutralino annihilations by a factor between 0.5 and 0.8 for  $m_\chi \leq 100 \text{ GeV}$  and by less than about 20% for higher masses for the oscillation parameters considered in this paper [34].

Recently the DAMA-NaI experiment observes a possible annual modulation effect in a WIMP direct search at a 99.6% C.L. [35]. This modulation has been interpreted in terms of a relic neutralino which may make up the major part of dark matter in the universe (see Ref. [36], and references therein). Figure 7 shows the allowed SUSY models considered by Bottino *et al.* for various neutralino local density compared to the MACRO upward-going muon flux limits from the Earth [36]. Bottino *et al.* model is basically the same as the one already described and shown in Figs. 5 and 6 limited to the subset of the parameter space which fulfills the DAMA result. MACRO experimental upper limits from the Earth rule out many SUSY configurations indicated by the DAMA-NaI experiment, even assuming the atmospheric neutrino background oscillates with the parameters favored by MACRO [23] and Superkamiokande [37]. On the other hand, the MACRO data from the Sun, which is more sensitive to spin-dependent scattering, has less sensitivity than direct searches at low masses. We again note that expected fluxes may decrease by at most a factor of 2 in the presence of neutrino oscillations.

## V. CONCLUSIONS

A search for a WIMP signal is performed using the MACRO detector at the Gran Sasso Laboratory to observe upward-going muons coming from the products of WIMP annihilations from the Earth and Sun. The time-of-flight

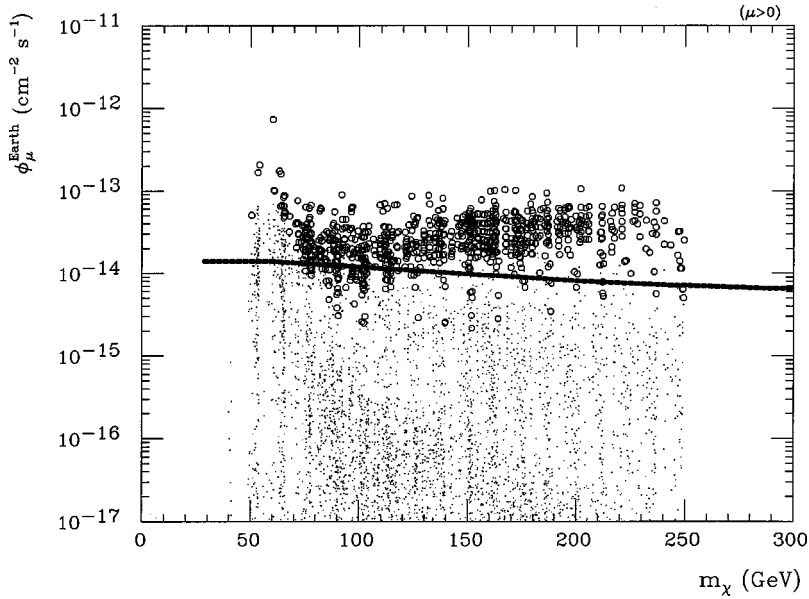


FIG. 5. Upward-going muon flux vs  $m_\chi$  for  $E_\mu^{\text{th}}=1$  GeV from the Earth [20]. Each dot is obtained varying model parameters. Dots correspond to variations of parameters between the following values:  $\tan \beta=1.01, 2, 3, 10, 40, 50$ ;  $m_A=65, 70, 75, 80, 85, 90, 95, 100, 200, 300, 500$  GeV, where  $m_A$  is the mass of the pseudoscalar Higgs;  $m_0=150, 200, 300, 500$  GeV, where  $m_0$  is the common soft mass of all the sfermions and squarks;  $A=-3, -1.5, 0, 1.5, 3$ , where  $A$  is the common value of the trilinear coupling in the superpotential for the bottom and top quark ( $A$  is set to zero for the first and second family);  $|\mu|$  and  $M_2$  are varied between 10 and 500 GeV in steps of 20 GeV. In this plot values of  $\mu>0$  are considered. Similar results are obtained for  $\mu<0$ . Solid line: MACRO flux limit (90% C.L.). The solid line representing the flux limit for the no-oscillation hypothesis is indistinguishable in the log scale from the one for the  $\nu_\mu-\nu_\tau$  oscillation hypothesis, but the expectations could be about two times lower. The dots and circles above the solid line are models excluded by MACRO upper limit. The open circles indicate the models excluded by direct measurements (particularly the DAMA-NaI experiment [38]) and assume a local dark matter density of  $0.5 \text{ GeV cm}^{-3}$ . See Fig. 7 for the comparison for the same density between the MACRO flux limit and the allowed values of parameters based on recent DAMA-NaI results.

technique is used to discriminate the upward-going neutrino-induced events from the background of downward-going atmospheric muons.

We look for an excess of neutrino events over the background of atmospheric neutrinos in the direction of the Sun and Earth. No signal of WIMP annihilation is observed, and

we present upper limits on the flux of upward-going muons from these bodies.

While we do not see a WIMP signal, we compare our flux limits to predictions from various SUSY models and rule out those which are inconsistent with our limits. We calculate the expected upward-going muon fluxes and angular distri-

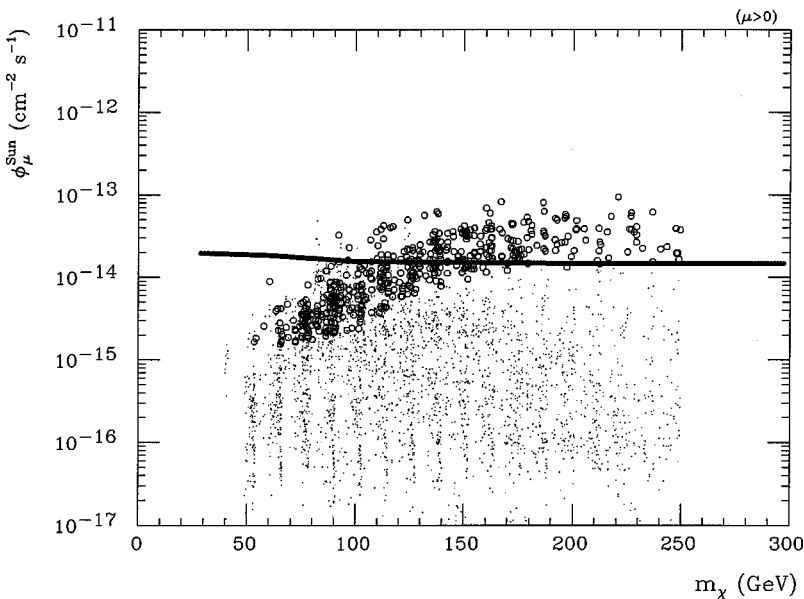


FIG. 6. Upward-going muon flux vs  $m_\chi$  for  $E_\mu^{\text{th}}=1$  GeV from the Sun [20]. Dots correspond to variations of parameters between the ranges described in the caption of Fig. 5. In this plot values of  $\mu>0$  are considered. Solid line: MACRO flux limit (90% C.L.). The open circles concern the regions excluded by direct measurements [38]. The dots and circles above the solid line are models excluded by MACRO upper limit.



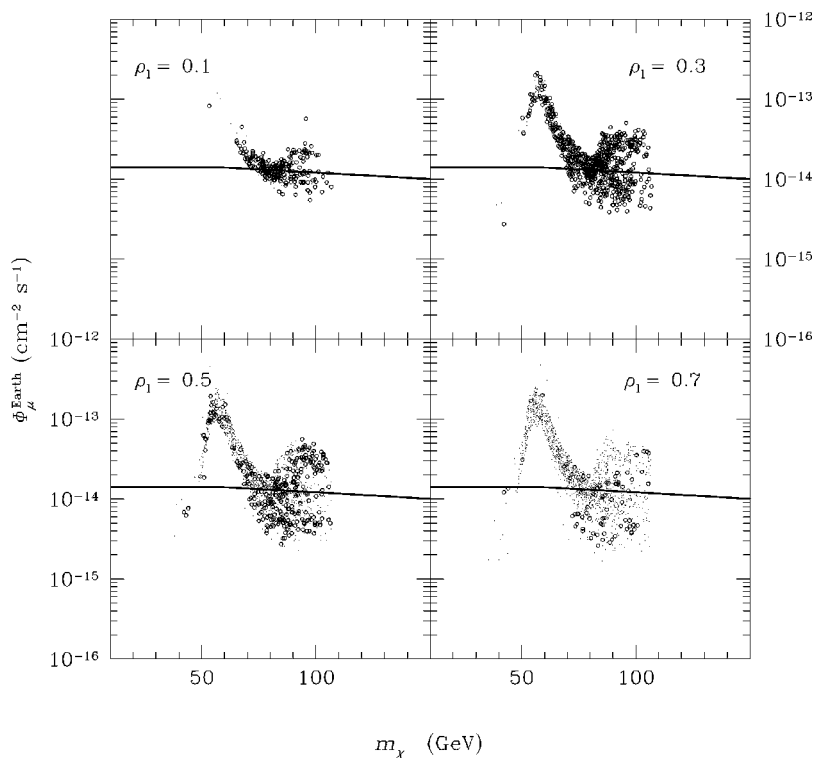


FIG. 7. Upward-going muon fluxes from the center of the Earth as a function of the neutralino mass. The solid lines are our experimental upgoing muon flux limits (for  $E_{\mu}^{\text{th}}=1$  GeV) at 90% C.L. as a function of  $m_{\chi}$  for the Earth. The dots and the circles are SUSY neutralino models from Bottino *et al.* [36] singled out by the DAMA-NaI indication of a possible annual modulation effect [35]. The plots are obtained assuming the indicated values of  $\rho_l$ , local dark matter densities in units  $\text{GeV}/\text{cm}^3$ . The experimental flux limit and the theoretical fluxes shown are obtained assuming no neutrino oscillations. The limits computed assuming oscillations are indistinguishable in these graphs; the expected fluxes may decrease by at most a factor of 2. The dots represent models already excluded by cosmic antiproton data [39].

butions using the SUSY neutralino annihilation calculations of Bottino *et al.* [20]. The 90% C.L. upper limits for the flux of upward-going muons in angular cones collecting 90% of the expected signal from neutralino annihilation are given. Our data exclude significant portions of the parameter space for neutralinos and our limits for the Earth are the most stringent of all “indirect” experiments [15,16]. The flux limits for the Sun, however, tend to rule out a smaller portion of the SUSY parameter space at this time. Finally, these data have also been able to exclude some of the SUSY models suggested by the annual modulation analysis performed by the DAMA-NaI experiment (especially at lower neutralino masses) [35].

#### ACKNOWLEDGMENTS

We thank Professor A. Bottino and N. Fornengo for valuable discussions and for their contributions to this work. We gratefully acknowledge the staff of the Laboratori Nazionali del Gran Sasso and the invaluable assistance of the technical staffs of all the participating Institutions. For generous financial contributions we thank the U.S. Department of Energy, the National Science Foundation, and the Italian Istituto Nazionale di Fisica Nucleare, both for direct support and for FAI grants awarded to non-Italian MACRO Collaborators.

- 
- [1] J. R. Primack, in *Dark Matter in Astro- and Particle Physics*, edited by H. V. Klapdor-Kleingrothaus and Y. Ramachers (World Scientific, Singapore, 1997), p. 97.
  - [2] A. Dekel and M. J. Rees, *Astrophys. J.* **422**, L1 (1994).
  - [3] K. A. Olive, in *Dark Matter in Astro- and Particle Physics* [1], p. 250.
  - [4] G. F. Smoot *et al.*, *Astrophys. J.* **396**, L1 (1992); C. L. Bennett *et al.*, *ibid.* **464**, L1 (1996).
  - [5] M. Persic, P. Salucci, and F. Stel, *Mon. Not. R. Astron. Soc.* **281**, 27 (1996).
  - [6] J. P. Ostriker and P. J. E. Peebles, *Astrophys. J.* **186**, 467 (1973).
  - [7] C. Alcock *et al.*, *Astrophys. J.* **486**, 697 (1997).
  - [8] G. Jungman, M. Kamionkowski, and K. Griest, *Phys. Rep.* **267**, 195 (1996).
  - [9] H. E. Haber and G. L. Kane, *Phys. Rep.* **117**, 75 (1985).
  - [10] OPAL Collaboration, K. Ackerstaff *et al.*, *Eur. Phys. J. C* **2**, 213 (1998); ALEPH Collaboration, R. Barate *et al.*, *ibid.* **2**, 417 (1998).
  - [11] K. Freese, *Phys. Lett.* **167B**, 295 (1986).
  - [12] L. Krauss, M. Srednicki, and F. Wilczek, *Phys. Rev. D* **33**, 2079 (1986).
  - [13] J. Silk, K. A. Olive, and M. Srednicki, *Phys. Rev. Lett.* **55**, 257 (1985).
  - [14] A. Gould, *Astrophys. J.* **321**, 571 (1987).
  - [15] BAKSAN Collaboration, M. M. Boliev *et al.*, *Nucl. Phys. B (Proc. Suppl.)* **48**, 83 (1996); in *Dark Matter in Astro- and Particle Physics* [1], p. 706.
  - [16] KAMIOKANDE Collaboration, M. Mori *et al.*, *Phys. Rev. D* **48**, 5505 (1993).

- [17] IMB Collaboration, J. M. LoSecco *et al.*, Phys. Lett. B **188**, 388 (1987).
- [18] A. Bottino, N. Fornengo, G. Mignola, and L. Moscoso, Astropart. Phys. **3**, 65 (1995).
- [19] L. Bergström, J. Edsjö, and P. Gondolo, Phys. Rev. D **55**, 1765 (1997).
- [20] A. Bottino, N. Fornengo, F. Donato, and S. Scopel (private communication); N. Fornengo, in the *Proceedings of the Ringberg Euroconference New Trends in Neutrino Physics*, Ringberg Castle, Tegernsee, Germany, May, 1998, edited by B. Kniel (World Scientific, Singapore, 1999). p. 319.
- [21] MACRO Collaboration, S. P. Ahlen *et al.*, Nucl. Instrum. Methods Phys. Res. A **324**, 337 (1993).
- [22] MACRO Collaboration, S. P. Ahlen *et al.*, Phys. Lett. B **357**, 481 (1995).
- [23] MACRO Collaboration, M. Ambrosio *et al.*, Phys. Lett. B **434**, 451 (1998).
- [24] MACRO Collaboration, M. Ambrosio *et al.*, Astropart. Phys. **9**, 105 (1998).
- [25] V. Agrawal, T. K. Gaisser, P. Lipari, and T. Stanev, Phys. Rev. D **53**, 1314 (1996).
- [26] J. G. Morfin and W. K. Tung, Z. Phys. C **52**, 13 (1991).
- [27] W. Lohmann *et al.*, CERN Yellow Report No. CERN-EP/85-03, 1985 (unpublished).
- [28] MACRO Collaboration, M. Ambrosio *et al.*, Phys. Rev. D **52**, 3793 (1995).
- [29] P. Lipari and M. Lusignoli, Phys. Rev. D **57**, 3842 (1998).
- [30] Particle Data Group, C. Caso *et al.*, Eur. Phys. J. C **3**, 1 (1998).
- [31] P. Lipari, M. Lusignoli, and F. Sartogo, Phys. Rev. Lett. **74**, 4384 (1995).
- [32] P. Lipari and T. Stanev, Phys. Rev. D **44**, 3543 (1991).
- [33] K. Griest and D. Seckel, Nucl. Phys. **B283**, 681 (1987).
- [34] N. Fornengo, *Proceedings of the International Workshop "Weak Interactions and Neutrinos (WIN99)"*, Cape Town, South Africa, January 1999, edited by C. A. Dominguez and R. D. Viollier (unpublished); hep-ph/9904351, 1999.
- [35] R. Bernabei *et al.*, Phys. Lett. B **424**, 195 (1998); **450**, 448 (1999).
- [36] A. Bottino, N. Fornengo, F. Donato, and S. Scopel, Astropart. Phys. **10**, 203 (1999).
- [37] Superkamiokande Collaboration, Y. Fukuda *et al.*, Phys. Rev. Lett. **81**, 1562 (1998).
- [38] R. Bernabei *et al.*, Phys. Lett. B **389**, 757 (1996).
- [39] BESS Collaboration, H. Matsunaga *et al.*, in the *Proceedings of the 25<sup>th</sup> International Conference of Cosmic Rays*, Durban, South Africa, 1997, edited by M. S. Potgieter, B. C. Raubenheimer, and D. J. van der Walt (Space Research Unit, 1997), Vol. 3, OG Sessions 1-5, p. 373.